*Human Brain Mapping*

WILEY

RESEARCH ARTICLE OPEN ACCESS

# Subcortical Hubs of Brain Networks Sustaining Human Consciousness

Morgan K. Cambareri[1,2] | Andreas Horn[1,3,4] | Laura D. Lewis[5,6,7] | Jian Li[1,7] | Brian L. Edlow[1,7]

[1]Department of Neurology, Center for Neurotechnology and Neurorecovery, Massachusetts General Hospital and Harvard Medical School, Boston, Massachusetts, USA | [2]Department of Biomedical Engineering, Boston University, Boston, Massachusetts, USA | [3]Center for Brain Circuit Therapeutics, Brigham and Women's Hospital, Massachusetts General Hospital, Boston, Massachusetts, USA | [4]Institute for Network Stimulation, Department of Stereotactic and Functional Neurosurgery, University Hospital Cologne, Germany | [5]Department of Electrical Engineering and Computer Science, Massachusetts Institute of Technology, Cambridge, Massachusetts, USA | [6]Institute for Medical Engineering and Science, Massachusetts Institute of Technology, Boston, Massachusetts, USA | [7]Department of Radiology, Athinoula A. Martinos Center for Biomedical Imaging, Massachusetts General Hospital and Harvard Medical School, Boston, Massachusetts, USA

**Correspondence:** Brian L. Edlow (bedlow@mgh.harvard.edu)

**Received:** 13 June 2025 | **Revised:** 29 August 2025 | **Accepted:** 4 September 2025

**Funding:** This work was supported by Tiny Blue Dot Foundation; National Institute of Neurological Disorders and Stroke, R01NS138257, R21NS109627, R21NS123412, R01NS127892, UM1NS132358, U19NS128613; NIH Office of the Director, DP2HD101400; National Institute on Aging, R01AG070135; National Institute of Mental Health, R01MH130666, R01MH113929; NIH BRAIN Initiative, U19NS128613; U.S. Department of Defense, CDMRP HT9425-24-1-1081; The Chen Institute MGH Research Scholar Award, MIT/MGH Brain Arousal State Control Innovation Center (BASCIC) project, Schilling Foundation, German Research Foundation (Deutsche Forschungsgemeinschaft, 424778381 – TRR 295), Deutsches Zentrum für Luft-und Raumfahrt (DynaSti grant within the EU Joint Programme Neurodegenerative Disease Research, JPND), and New Venture Fund (FFOR Seed Grant).

## ABSTRACT

Neuromodulation of subcortical network hubs by pharmacologic, electrical, or ultrasonic stimulation is a promising therapeutic strategy for patients with disorders of consciousness (DoC). However, optimal subcortical targets for therapeutic stimulation are not well established. Here, we leveraged 7 Tesla resting-state functional MRI (rs-fMRI) data from 168 healthy subjects from the Human Connectome Project to map the subcortical connectivity of six canonical cortical networks that modulate higher-order cognition and function: the default mode, executive control, salience, dorsal attention, visual, and somatomotor networks. Based on spatiotemporally overlapped networks generated by the Nadam-Accelerated SCAlable and Robust (NASCAR) tensor decomposition method, our goal was to identify subcortical hubs that are functionally connected to multiple cortical networks. We found that the ventral tegmental area (VTA) in the midbrain and the central lateral and parafascicular nuclei of the thalamus—regions that have historically been targeted by neuromodulatory therapies to restore consciousness—are subcortical hubs widely connected to multiple cortical networks. Further, we identified a subcortical hub in the pontomesencephalic tegmentum that overlapped with multiple reticular and extrareticular arousal nuclei and that encompassed a well-established "hot spot" for coma-causing brainstem lesions. Multiple hubs within the brainstem arousal nuclei and thalamic intralaminar nuclei were functionally connected to both the default mode and salience networks, emphasizing the importance of these cortical networks in integrative subcortico-cortical signaling. Additional subcortical connectivity hubs were observed within the caudate head, putamen, amygdala, hippocampus, and bed nucleus of the stria terminalis, regions classically associated with modulation of cognition, behavior, and sensorimotor function. Collectively, these results suggest that multiple subcortical hubs in the brainstem tegmentum, thalamus, basal ganglia, and medial temporal lobe modulate cortical function in the human brain. Our findings strengthen the evidence for targeting subcortical hubs in the VTA, thalamic

The last two authors are co-senior authors.

intralaminar nuclei, and pontomesencephalic tegmentum to restore consciousness in patients with DoC. We release the subcortical connectivity maps to support ongoing efforts at therapeutic neuromodulation of consciousness.

## 1 | Introduction

Human consciousness requires functional connections between subcortical and cortical networks that mediate arousal and awareness, respectively (Edlow et al. 2024; Koch et al. 2016). In patients with severe brain injuries, the reintegration of connectivity between subcortical and cortical networks is essential for recovery of consciousness (Edlow, Claassen, et al. 2021). However, there are currently few therapies proven to promote recovery of consciousness in patients with severe brain injuries (Giacino et al. 2012), a limitation in clinical care that is partly attributable to a lack of therapeutic targets (Edlow, Sanz, et al. 2021). To identify such targets, it is essential to generate a reliable map of subcortico–cortical connectivity in the healthy, conscious human brain, as this map may be used to guide the search for widely connected network hubs that could be stimulated to restore consciousness in the injured brain.

Growing evidence suggests that widely connected network hubs play a key role in higher-level cognitive functions (van den Heuvel and Sporns 2013) and that disconnection of network hubs is implicated in the pathogenesis of a broad range of neuropsychiatric disorders (Crossley et al. 2014). In patients with disorders of consciousness (DoC), the relevance of network hubs to the loss and restoration of consciousness is supported by human studies showing that hub lesions cause coma (Edlow et al. 2013; Fischer et al. 2016; Parvizi and Damasio 2003) and that hub stimulation may promote the reemergence of consciousness (Giacino et al. 2012; Schiff et al. 2007). Animal models have similarly revealed that focal lesions within the brainstem tegmentum (Fuller et al. 2011; Pais-Roldan et al. 2019) and targeted stimulation within the central thalamus (Redinbaugh et al. 2020; Tasserie et al. 2022) may cause loss and restoration of consciousness, respectively, under a variety of experimental conditions. Consistent with these animal models, clinical trials in humans with DoC have historically targeted subcortical hubs in the central thalamus (Cain, Spivak, et al. 2021; Cain et al. 2022; Schiff et al. 2007), brainstem tegmentum (Edlow et al. 2020; Elias et al. 2021; Fridman et al. 2019; Giacino et al. 2012), and basal ganglia (Cain, Visagan, et al. 2021; Whyte et al. 2014).

A barrier to progress in therapeutic target selection for humans is that there are gaps in knowledge about how subcortical hubs modulate their cortical counterparts in the healthy, conscious human brain. While extensive progress has been made in understanding this physiology in animals (Aston-Jones et al. 2001; Moruzzi and Magoun 1949; Scammell et al. 2017; Steriade and Glenn 1982; Vertes and Martin 1988) via electrophysiological, lesion-based, and tract-tracing studies, the physiology of subcortical networks has not been fully elucidated in humans. Specifically, it is unknown which subcortical hubs activate cortical networks, inhibit cortical networks, or mediate state switches. Identifying integrative network hubs that link arousal and awareness may reveal the subcortical targets that are most likely to promote recovery of consciousness in patients with DoC.

Advances in functional MRI (fMRI) (Luppi et al. 2024) and the availability of large normative datasets as part of the Human Connectome Project (HCP) (Glasser et al. 2016; Smith et al. 2013) now create opportunities to identify subcortical network hubs and elucidate the mechanisms by which they modulate human consciousness, providing new therapeutic target candidates for patients with DoC. Here, we aimed to identify the subcortical regions of the human brain that possess high levels of functional connectivity with multiple cortical networks—regions that we define as subcortical network hubs. While this approach to functional connectivity mapping cannot determine the direction of electrical signaling between subcortical and cortical regions, there is evidence that stimulating small subcortical regions is an effective strategy for activating multiple cortical networks via diffuse ascending connections (Horn and Fox 2020).

Using the Nadam-Accelerated SCAlable and Robust (NASCAR) decomposition method on the resting-state fMRI (rs-fMRI) data from 168 HCP healthy subjects, we generated subcortical functional connectivity maps for six canonical large-scale brain networks. We identified subcortical hubs that strongly connect to multiple cortical networks by measuring the overlaps in functional connectivity maps within the subcortical regions. Further, we characterized the functional connectivity properties by which subcortical hubs interact with cortical networks (i.e., correlated versus anticorrelated functional connectivity). We release all functional connectivity maps to support progress in the field of human brain mapping and to inform the design of future clinical trials aimed at neuromodulation of consciousness.

## 2 | Materials and Methods

### 2.1 | 7 Tesla rs-fMRI Data

We analyzed the minimally preprocessed 7 Tesla (7 T) rs-fMRI healthy control data (Glasser et al. 2013) from the WashU/U Minn component of the HCP (Glasser et al. 2016). Of the 178 subjects with rs-fMRI scans in the dataset, only 168 were included due to reported acquisition and preprocessing issues in 8 subjects. Each rs-fMRI dataset was collected in four independent 15-min sessions using a gradient-echo EPI sequence (1.6 mm isotropic voxels, TE = 22.2 ms, TR = 1000 ms) with opposite phase encoding directions (AP, PA). As the distinct phase-encoding directions introduce different spatial distortions, we used the first session with PA phase encoding direction to minimize inter-subject misalignment, consistent with recent work (Li, Curley, et al. 2021). To evaluate this approach, we performed a reliability test (Figure S1 and Table S1) that showed highly reproducible components between networks identified in the first session and those identified from the two sessions combined. These data were coregistered to the MNI 152 6th-generation space and represented in CIFTI grayordinate space with 91,282 total cortical and subcortical vertices/voxels (approximately 30 K vertices per hemisphere cortically and an additional 30 K voxels in the subcortex) as part of the HCP minimal preprocessing pipeline

(Glasser et al. 2013). Aside from the 2 mm FWHM Gaussian smoothing kernel applied during the minimally preprocessed pipeline, no additional smoothing was applied to avoid blurring across different functional regions (Li et al. 2018). Before motion correction and spatial registration, the minimally preprocessed pipeline estimates a distortion field using FSL's TOPUP method, which corrects for field inhomogeneity and gradient coil specific distortions.

## 2.2 | Identification of Spatially Overlapped Brain Networks Using NASCAR

We used the NASCAR tensor decomposition method to identify large-scale brain networks. The key distinction between NASCAR and traditional seed-based methods (Lee et al. 2013) or parcellation schemes (Yeo et al. 2011) is that NASCAR allows networks to be spatially overlapped and temporally correlated. Unlike other commonly used data-driven approaches, such as independent component analysis (ICA) or principal component analysis (PCA), NASCAR does not impose independence or orthogonality constraints. There is growing evidence that fluctuations in functional connectivity temporally overlap rather than representing discrete states over time (Hutchison et al. 2013; Karahanoglu and Van De Ville 2015). Similarly, there is evidence for spatial overlap between resting state networks (Seeley et al. 2007; Leech et al. 2012). Furthermore, recent evidence suggests that networks identified by NASCAR are more physiologically plausible than those identified by ICA or PCA (Li et al. 2023; Li, Wisnowski, et al. 2021) and that subcortical functional connectivity identified by NASCAR closely corresponds to gold-standard histopathology (Li, Curley, et al. 2021). The allowance of spatial overlap between networks enables the identification of subcortical network hubs, which are defined as regions that participate in multiple cortical networks.

### 2.2.1 | Temporal Synchronization Using Group BrainSync

Prior to NASCAR, an inter-subject temporal synchronization method, "BrainSync" (Joshi et al. 2018), was performed to align the rs-fMRI signals across subjects. This step was necessary as rs-fMRI data reflect spontaneous brain activity and are not synchronous between subjects. To account for potential bias in the synchronization target, we used the group version of the BrainSync algorithm (Akrami et al. 2019), creating a virtual reference subject, which is, on average, close to all subjects in the population. Each subject's data was then temporally aligned to that virtual reference subject. Critically, this synchronization procedure does not change the subject connectivity profile, as it would be measured by spatial correlations. The group result can then be mapped back to the individual space using the invertibility property of the BrainSync algorithm.

### 2.2.2 | NASCAR Tensor Decomposition

The synchronized rs-fMRI data were concatenated along the subject dimension, forming a third-order tensor, which has a spatial dimension (number of total vertices/voxels) of $V = 91292$, a temporal dimension (number of time points) of $T = 900$, and a subject dimension (number of subjects) of $N = 168$. We ran NASCAR on this third-order tensor and obtained low-rank components representing large-scale brain networks common across all subjects.

## 2.3 | Identification and Classification of Functional Brain Network Hubs

### 2.3.1 | Identification of Whole-Brain Resting State Networks From the Cortical Maps

Each spatial map identified using the NASCAR method represents the spatial distribution of a whole-brain network consisting of both the cortical component and the subcortical component. Figure 1 shows an example network encoded in the CIFTI format. The network map was separated into two cortical (left and right hemispheres) and one subcortical component and mapped onto the surface and the volumetric space for visualization, respectively. We visually examined the cortical components and identified six canonical resting-state networks, all consistent with prior literature (Raichle 2011; Yeo et al. 2011): the default mode network (DMN), salience network (SN), executive control network (ECN), dorsal attention network (DAN), somatomotor network (SMN), and visual network (VN) (Figure S2). Although a potential limbic network with medial temporal and temporal pole

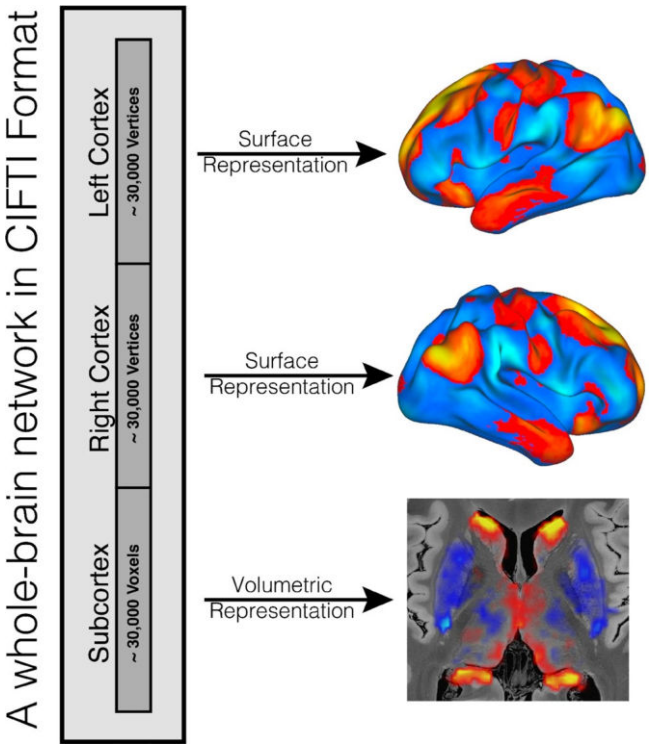


**FIGURE 1** | An example network (DMN) identified by the NASCAR method. The spatial map represented in the CIFTI format consists of both cortical and subcortical components. They were separated and mapped onto the surface and the volumetric space for visualization, respectively. All volumetric visualizations in Figure 1 and subsequent Figures are superimposed upon the 100 micron MRI template in MNI space (Edlow et al. 2019).

signals was visually identified, this component did not have connectivity within the orbitofrontal cortex, as previously reported in (Yeo et al. 2011). Additionally, a recent fMRI study suggested that the limbic network is part of the extended DMN rather than a separate and functionally distinct large-scale network (Girn et al. 2024). Therefore, we focused on the abovementioned six major large-scale networks and did not include a separate limbic network for the following analyses.

#### 2.3.2 | Separation of Subcortical Resting State Networks

For each network, we extracted the subcortical component (Figure 1, bottom) and converted it to a 3D volume. We then transformed this volume into the MNI NLIN 2009 space and linearly interpolated the map to 0.5 $mm^3$ resolution. We removed the cerebellar signal from the subcortical volumes for this study because the cerebellum is closer to the head coil and has a higher signal-to-noise ratio (Koike et al. 2021) compared to the subcortical structures we are focusing on in this work. Thus, it could introduce a strong bias toward the thresholding procedure below. Furthermore, while damage to the brainstem, thalamus, and basal ganglia has been associated with DoC, individuals with damage to the cerebellum (or born without a cerebellum) can sustain arousal and awareness (Lemon and Edgley 2010), which makes the cerebellum less therapeutically relevant in patients with DoC.

#### 2.3.3 | Identification of Subcortical Resting State Network Hubs

Our first goal was to identify subcortical nodes whose BOLD signal was correlated or anticorrelated with multiple cortical networks. We identified the "correlated network hubs" as follows: We first binarized the subcortical map for each individual network by thresholding their distribution to preserve only the top 5% of values and then superimposed the six binarized maps. We identified the "anticorrelated network hubs" similarly using the bottom 5% threshold. Mixed hubs were identified by combining the results from the correlated and anticorrelated network hub overlaps. See Table 1 for the full descriptions of each hub type.

In addition to visualizing the neuroanatomic overlap of binarized network maps, we measured the "hubness" at each voxel by summing how many networks "passed" (above for correlated hubs and below for anticorrelated hubs) the 5% threshold (i.e., accumulating the binary masks across networks). This created a discrete hub map with values ranging from 0 to 6 ("0" means no network survived the 5% thresholding at this location, and "6" means all networks survived). We repeated this hubness measure for anticorrelated network maps. Furthermore, we identified subcortical nodes whose BOLD signal was highly connected to multiple cortical networks regardless of sign (correlated or anticorrelated). To do so, we measured the hubness using the binarized "mixed hub" maps and summed the number of networks falling into either the top 5% or the bottom 5% of the distribution at each voxel.

#### 2.3.4 | Network Threshold Contours

To provide a more granular and contiguous view of the network hubs, we approached the same question from a different perspective. For a fixed $k$ number of networks at each voxel, we queried the highest threshold that could be used to binarize the network maps such that there are $k$ networks overlapped at this location. We refer to these continuously valued threshold maps as "contour maps" hereafter. In this analysis, different network combinations could occur at different locations. We use $k = 4$ for visualization trade-off to illustrate the consistency and correspondence between our hubness results and regions historically associated with consciousness level. All images in this paper are shown in radiological convention where the left hemisphere is shown on the right side of the image and vice versa.

## 3 | Results

### 3.1 | Visualization of Subcortical Resting State Networks

Figure 2 shows the subcortical maps of six canonical resting-state networks identified by the NASCAR decomposition method at axial slices through the pons, midbrain,

**TABLE 1** | Classification of three types of network hubs.

| Classification | Description |
|---|---|
| "Correlated" network hubs | Each network map was thresholded to preserve the top 5% of its most correlated voxels within the subcortex (i.e., the top 5% of the distribution), creating a binary network mask. The correlated network masks were overlapped with one another to identify subcortical regions that are highly correlated to multiple cortical networks. |
| "Anticorrelated" network hubs | Each network map was thresholded to preserve the top 5% of its most anticorrelated voxels within the subcortex (i.e., the bottom 5% of the distribution), creating a binary network mask. The anticorrelated network masks were overlapped with one another to identify subcortical regions that are highly anticorrelated to multiple cortical networks. |
| "Mixed" network hubs | Each network map was thresholded to preserve the top 5% of its most correlated and anticorrelated voxels within the subcortex (i.e., both the top 5% and bottom 5% of the distribution), creating a single mixed binary network mask. The mixed network masks were overlapped with one another to identify subcortical regions that have strong relationships to multiple cortical networks but with mixed signs. |

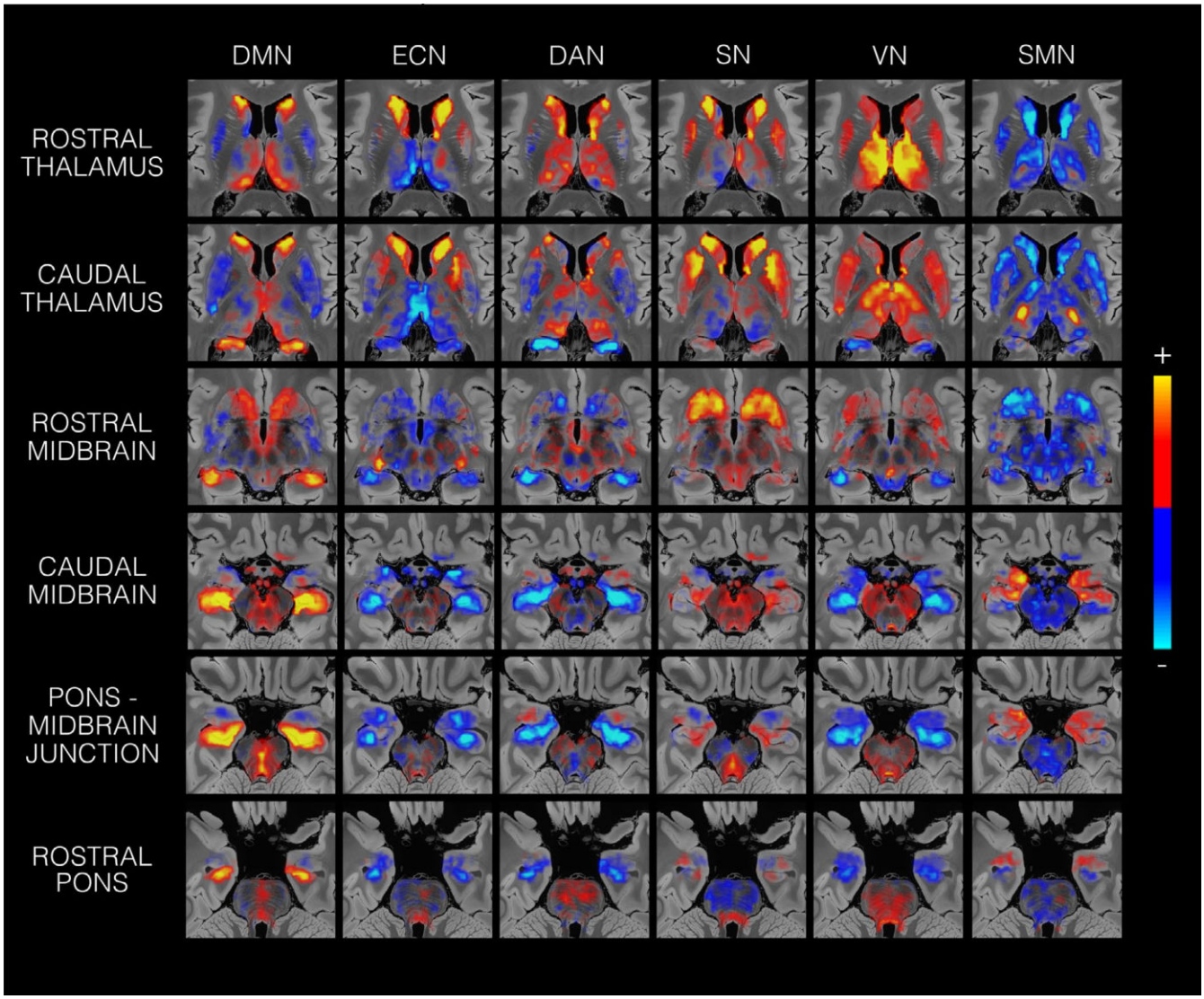


**FIGURE 2** | Subcortical connectivity profiles of six canonical networks. The networks are the default mode network (DMN), executive control network (ECN), dorsal attention network (DAN), salience network (SN), visual network (VN), and somatomotor network (SMN), shown at descending axial slices. All maps are in the radiological convention. For reference, approximate anatomical locations for each axial slice are depicted in Figure S6.

diencephalon, basal forebrain, and basal ganglia. These network maps are available at https://github.com/ComaRecoveryLab/Subcortical_Network_Hubs. Visual inspection revealed that the networks were mostly symmetric across the midline of the brain, with occasional hemispheric differences in the connectivity profile.

We observed heterogeneous patterns of network connectivity across the subcortex, as cortical networks had distinct mixtures of correlations and anticorrelations within subcortical regions. For example, the ECN showed correlations with the basal ganglia but anticorrelations within the thalamus and medial temporal lobe. These heterogeneities were also seen within individual regions of interest, with many nuclei having diverse patterns of connectivity. For example, the rostral putamen was highly correlated with the ECN and DAN, whereas the caudal putamen was anticorrelated. Additionally, the distribution of connectivity was not consistent across networks, as some networks tended to show more subcortical anticorrelations and some more subcortical correlations. For example, the SMN showed mostly anticorrelations within the subcortex, with only a few small regions of high positive correlations, such as in the amygdala and the ventral posterolateral thalamic nucleus (VPL).

### 3.2 | Correlated and Anticorrelated Regions

Figure 3 shows the most correlated subcortical regions for each network. In the final "Combined" column of these panels, the most correlated (thresholded to preserve the top 5% of values for each network) masks were overlapped to visualize regions of network integration.

Figure 3 shows the regions with highly correlated network overlap within the caudate head and the bed nucleus of the stria terminalis (BNST). Networks that overlapped within the caudate head were the DMN, SN, ECN, and SN. The VN additionally

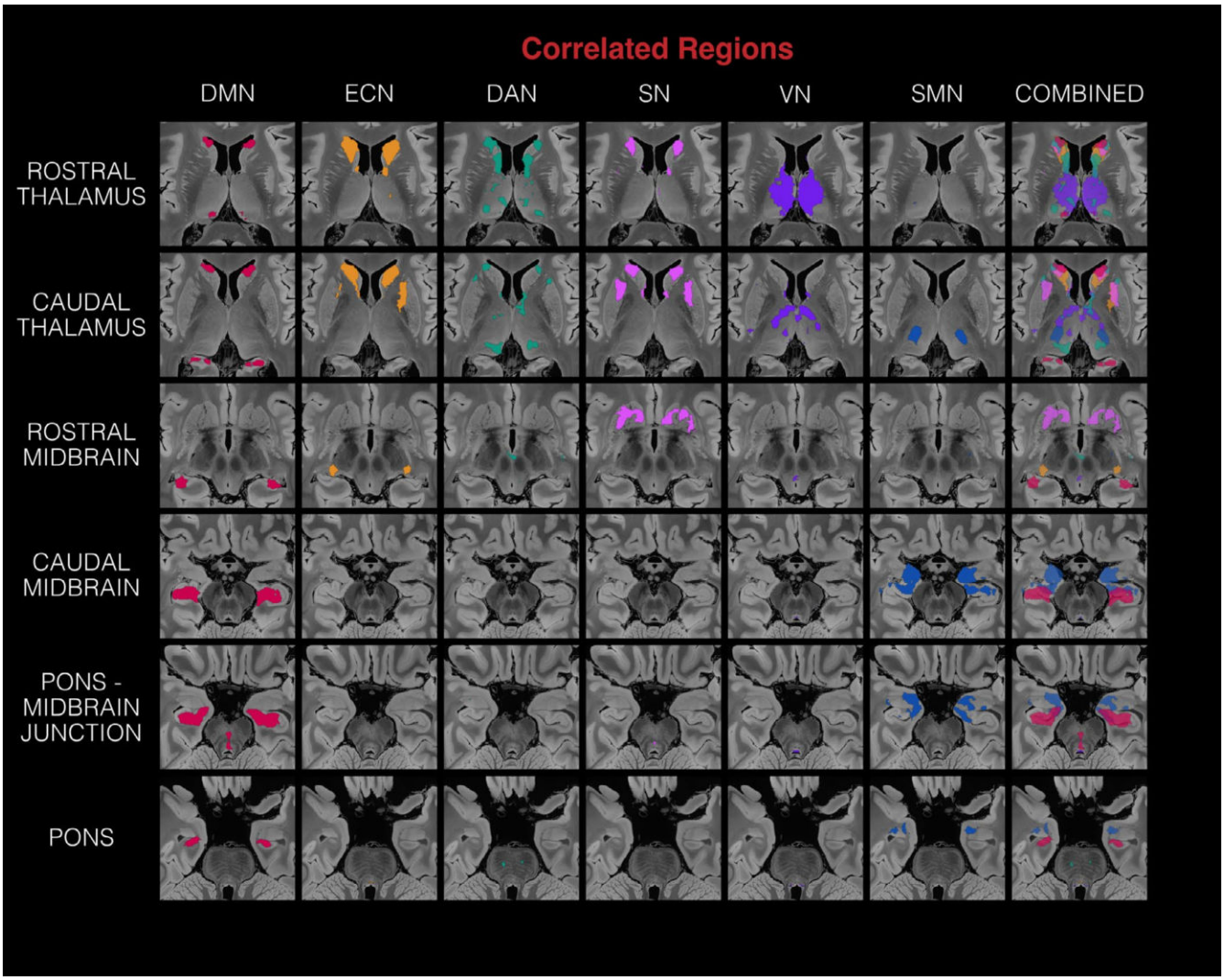


**FIGURE 3** | Correlated regions for each network. Each column (except for the last one) represents an individual network, and the colored voxels represent voxels within the top 5% (or the most correlated) of values for that network within the entire subcortex. The last column shows the combination (semi-transparent overlap) of individual network maps.

overlapped with the SN, ECN, and the DAN within the BNST and the DAN within the thalamus.

Figure 4 is the counterpart to Figure 3, with the thresholding performed to preserve the bottom 5% of values for each network. Figure 4 shows the regions with highly anticorrelated network overlap within the amygdala and the hippocampus. We found that the networks most overlapped within the hippocampus were the DAN, SN, and VN. The DMN, ECN, SN, and VN additionally had a small overlap region within the amygdala. While there were notably few regions of overlap within basal ganglia, thalamic, and brainstem structures, there were slight overlaps between the ECN and SN, as well as the ECN and SMN, within the rostral and caudal thalamus.

### 3.3 | Correlated, Anticorrelated, and Mixed Network Hubs

Regions with multiple network overlaps are shown in Figure 5, which provides an overview of "correlated network hubs," "anticorrelated network hubs," and "mixed network hubs." In the "correlated" condition (the first pair of columns), the left column defines the number of network overlaps for all six thresholded correlated masks in Figure 3. For reference, the right column shows the combined map from the last column of Figure 3, indicating the identities of the networks that are overlapping. The middle column pair shows the counterpart for the anticorrelated condition, where the thresholding preserves the bottom 5% of values for each network. For the "mixed network hub" condition in the last column pair, we combined the masks from both the "correlated" and "anticorrelated" conditions.

We observed two main regions of correlated network hubs within the caudate head and the BNST, where four networks overlapped. The networks overlapping at these two regions were the DMN, ECN, DAN, and SN for the caudate head and the ECN, DAN, SN, and VN for the BNST. We also observed two regions of anticorrelated network hubs within the amygdala and the hippocampus, with four and three networks overlapping, respectively. The networks overlapping in these two regions were

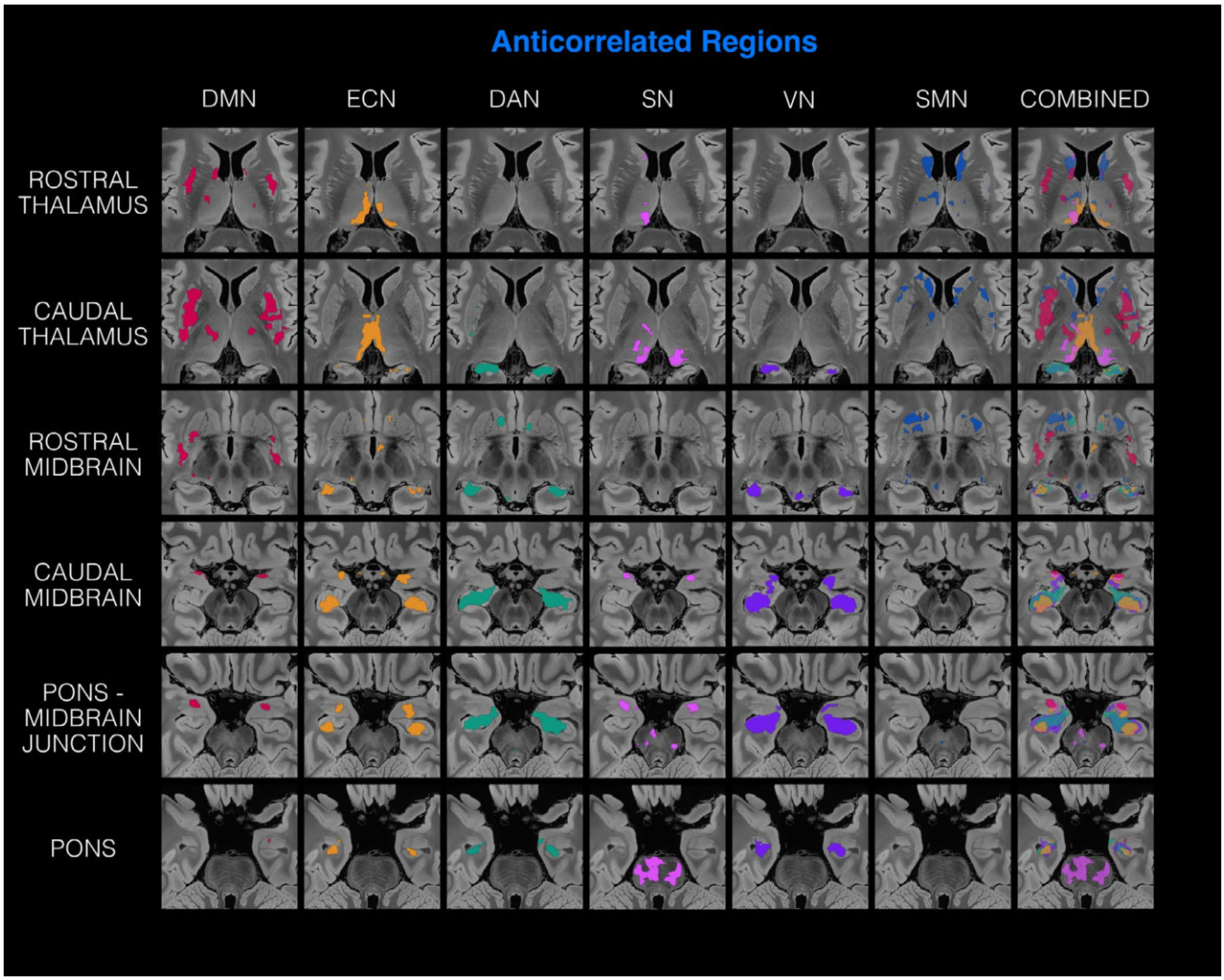


**FIGURE 4** | Anticorrelated regions for each network. Each column (except for the last one) represents an individual network, and the colored voxels represent voxels within the bottom 5% (or the most anticorrelated) of values for that network within the entire subcortex. The last column shows the combination (semi-transparent overlap) of individual network maps.

the DMN, ECN, and SN and VN for the amygdala and the ECN, DAN, and VN for the hippocampus.

When we combined the correlated and anticorrelated network masks to identify mixed network hubs, we identified regions with more heterogeneous relationships to resting-state networks. We identified that a region within the caudate head not only had strong correlated relationships to four higher-order cognitive networks but was also anticorrelated to the SMN. The BNST was notably the only nucleus with strong relationships to all six networks within this "mixed" condition, with a strong correlated relationship to four networks (ECN, SN, DAN, and VN) and a strong anticorrelated relationship to two networks (DMN and SMN). A small unilateral region within the amygdala overlap increased to five networks within the mixed condition, as a correlated overlap with the SMN was added to its previous four anticorrelated network contributions. Within the hippocampus, there was a bilateral region of five network overlaps with the addition of two correlated networks (DMN and SMN) overlapping with three anticorrelated networks (ECN, DAN, VN).

### 3.4 | Regions Associated With Consciousness Level Correlate With Multiple Cortical Resting State Networks

Figures 6–8 describe network hubs within multiple subcortical regions that are associated with consciousness level. Network contour maps were generated for these three figures to identify the highest threshold necessary for there to be $k$ networks overlapped at each voxel. $k = 4$ was used to best illustrate the correspondence between the hubs identified in the present work and the hotspots identified in prior studies where lesions are associated with loss of consciousness (Fischer et al. 2016; Parvizi and Damasio 2003; Snider et al. 2020).

Figure 6 displays the 4-network correlated contour map findings within the CL thalamic nucleus in (A) left column and for the perifascicular thalamic nucleus (Pf) in (B) left column with the axial, sagittal, and coronal views from top to bottom. The right column in both (A) and (B) shows the probabilistic values for the CL and Pf nuclei as defined by the probabilistic thalamic segmentation

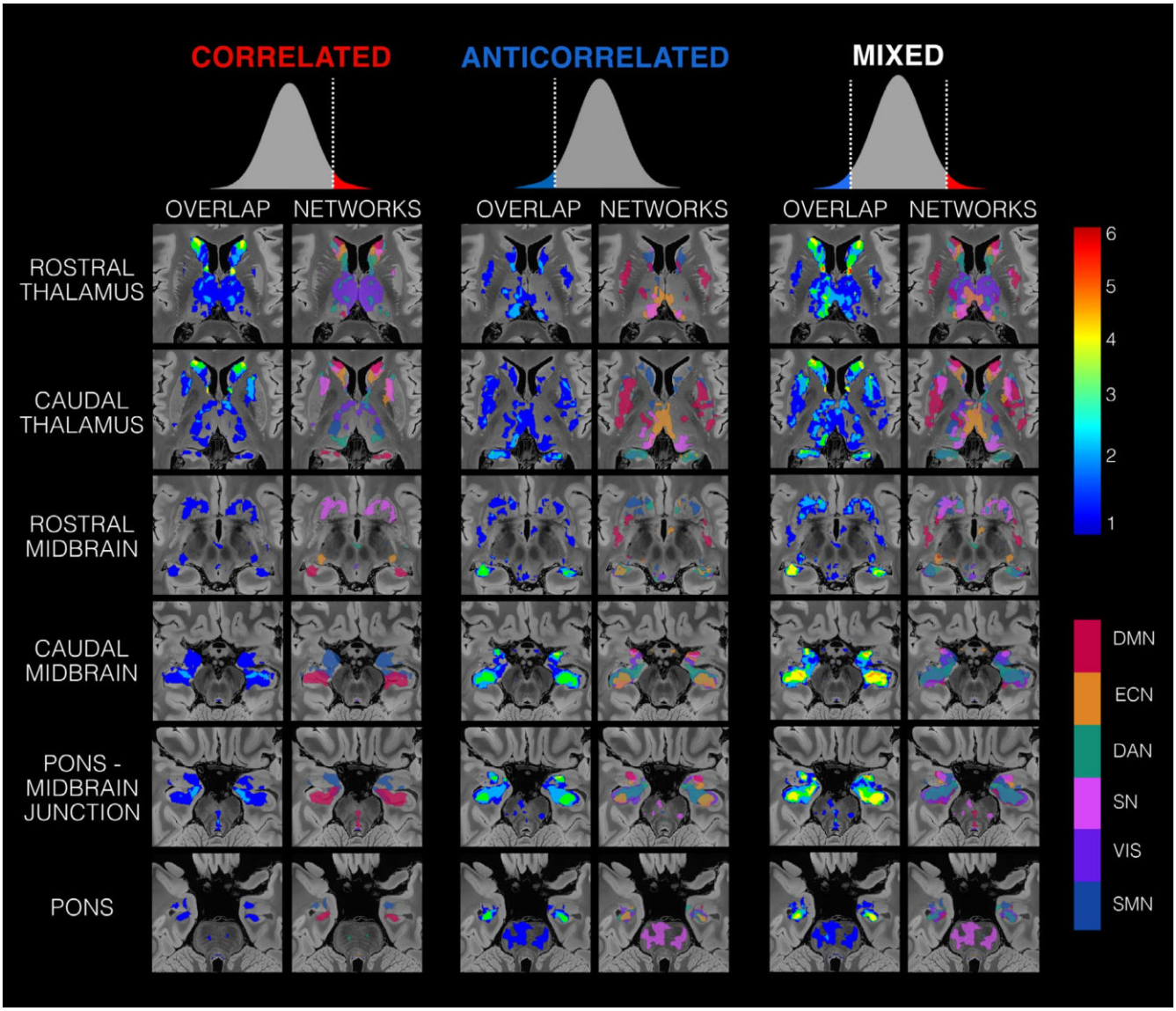


**FIGURE 5** | Network overlap and identity maps for the correlated (left column pair), the anticorrelated (middle column pair) and the mixed (right column pair) conditions shown in descending axial slices. The left column in each column pair shows the map describing the number of network overlaps at every voxel with values ranging from 0 to 6, as indicated by the top right color bar. The right column in each column pair labels the locations and identity of the thresholded networks overlapping at every voxel, where each color represents a distinct brain network as indicated by the bottom right color bar.

atlas (Iglesias et al. 2018). This distribution of probability values indicates where these nuclei are most likely to be defined in space. The anatomic borders of CL and the Pf in this atlas encompass the 4-network contour map, providing evidence that these thalamic intralaminar nuclei have high levels of network integration. For the left hemispheric CL, the networks overlapping were the DMN, DAN, SN, and VN. Notably, the right CL highly correlates with the DMN, DAN, and VN but is missing a contribution from the SN (Figure S4). The Pf finding was also asymmetrical, with a smaller profile on the right hemisphere than on the left. Within the left Pf, the networks overlapping were the DMN, ECN, DAN, and SN. The networks overlapping within the smaller spot in the right Pf were the DMN, DAN, SN, and VS.

Figure 7 displays network hubs within the brainstem that overlap with three previously reported brainstem "hot spots": two previously reported regions that cause coma when lesioned (Fischer et al. 2016; Parvizi and Damasio 2003) and one region whose connectivity to cortical lesions was associated with loss of consciousness (Snider et al. 2020). The first column shows the Parvizi hotspot superimposed on axial sections of the brainstem. The second and third columns show the Fischer and Snider hotspots (white outlines) superimposed on hub connectivity data from the present study. All three previously published hotspots overlap with our 4-network correlated hub within the pontomesencephalic tegmentum.

Figure 8 shows the axial, sagittal, and coronal slices from the midbrain to the pontine structures of the 4-network contour map alongside six ascending arousal network nuclei as defined by the Harvard Ascending Arousal Network (AAN) Atlas, version 2.0 (Edlow et al. 2024). Each panel describes the hotspots

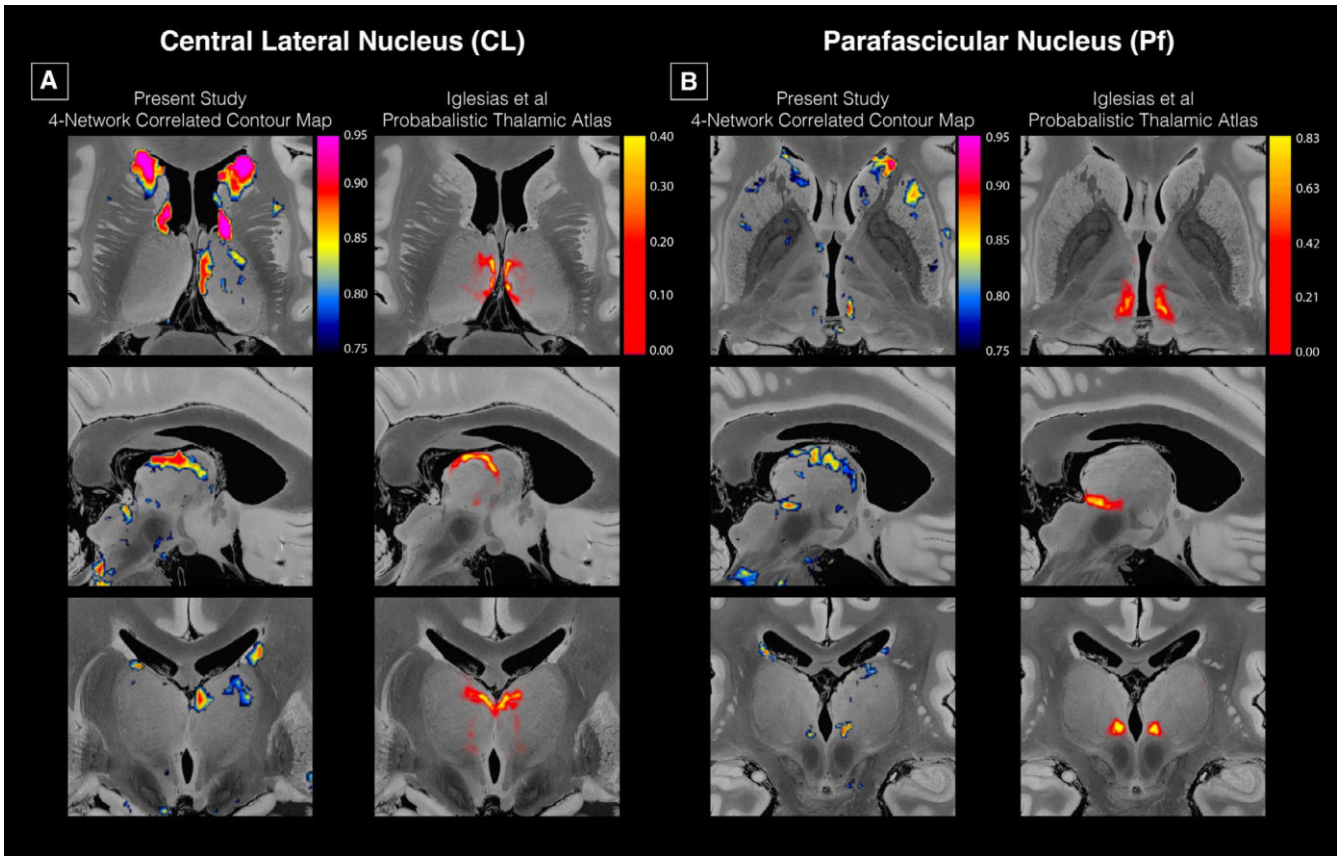


**FIGURE 6** | Subcortical correlated connectivity hubs within the central lateral (CL) and parafascicular (Pf) nuclei of the thalamus. (A) A comparison of the probabilistic thalamic segmentation atlas (Iglesias et al. 2018) for the CL thalamic nucleus alongside the 4-network correlated contour map is shown from an axial (top row), left hemispheric sagittal (middle row), and coronal (bottom row) perspective. (B) The counterpart to (A) but for the Pf.

in the 4-network contour map, where they overlap with the corresponding AAN nuclei in the left panel. We found that multiple AAN nuclei overlap with at least four correlated networks. There was a consistent pattern of multiple higher-order cognitive networks being positively correlated to multiple AAN nuclei. The SN, DMN, and VN were three of the four correlated networks for all these brainstem nuclei. A detailed summary of the relationships between the large-scale resting-state networks and the AAN nuclei is shown in Table 2.

## 4 | Discussion

This brain mapping study leveraged a 7T rs-fMRI healthy control dataset with 168 subjects and a tensor-based NASCAR decomposition method to map the subcortical connectivity of six canonical resting state networks. We identified multiple subcortical network hubs demonstrating differential patterns of functional connectivity with cortical networks. These hubs included regions that have been historically targeted in therapeutic stimulation studies of patients with DoC: the CL, Pf, and VTA (Chudy et al. 2018, 2023; Giacino et al. 2012; Schiff et al. 2007). In addition, we found a subcortical connectivity hub in a region of the pontomesencephalic tegmentum that overlaps with multiple reticular and extrareticular arousal nuclei and that has been shown in three prior lesion studies to be a "hot spot" associated with loss of consciousness (Fischer et al. 2016; Parvizi and Damasio 2003; Snider et al. 2020), strengthening the evidence that this region of the brainstem tegmentum is critical to human consciousness. All brainstem and thalamic hubs were functionally connected to both the DMN and SN, emphasizing the importance of these cortical networks in integrative subcortico-cortical signaling in the human brain. Furthermore, we identified subcortical hubs in the caudate head, putamen, hippocampus, amygdala, and BNST—regions that are classically associated with modulation of cognition, behavior, and sensorimotor function. Collectively, these observations provide insights into the subcortical regions of the human brain that are strongly coupled to large-scale cortical networks and identify potential targets for therapeutic neurostimulation studies aimed at promoting recovery of consciousness in patients with DoC.

Our subcortical connectivity findings add to the growing evidence base for a therapeutic paradigm in which subcortical regions are targeted to restore consciousness in patients with DoC. We identified multiple subcortical nodes that were connected to four cortical networks and a small number of subcortical nodes connected to as many as six cortical networks. For example, the caudate head was observed to be a 6-network correlated hub, and the BNST a 6-network mixed hub. Accordingly, stimulation of subcortical hub nodes has the potential to activate a broad expanse of cortical neurons across multiple functionally connected networks. In prior clinical trials, electrophysiologic stimulation of the central thalamus (Schiff et al. 2007) and

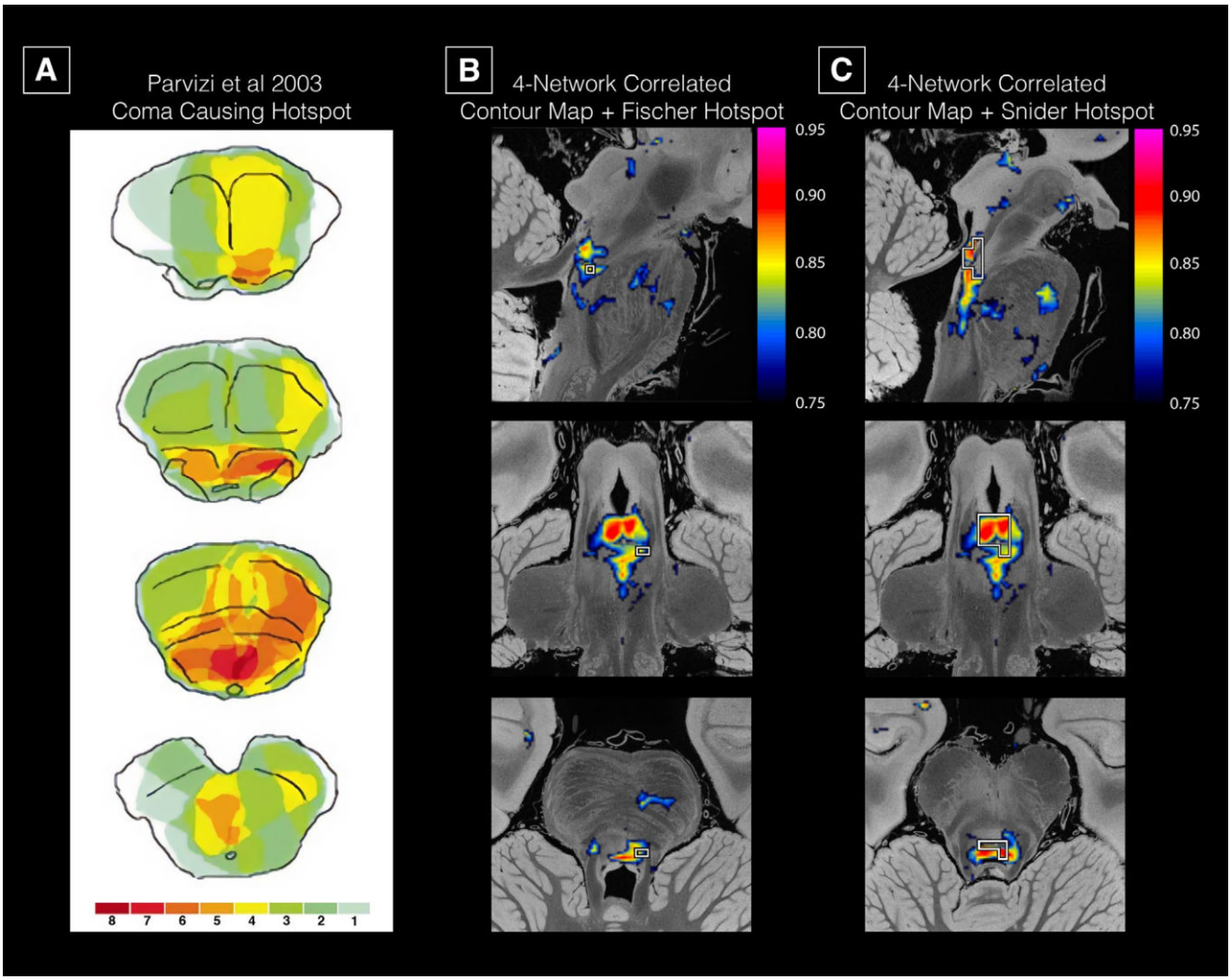


**FIGURE 7** | Brainstem tegmentum connectivity hub overlaps with regions previously implicated in modulating human consciousness. Panel (A) shows lesion locations within the brainstem in patients presenting with coma (figure adapted from Parvizi 2003). The colors correspond to the number of patients with lesions in that region. Panel (B) shows our 4-network correlated contour map with a white outline labeling the region of maximum lesion overlap from patients presenting with coma from Fischer et al. (2016). Panel (C) shows our 4-network correlated contour map with a white outline labeling another brainstem hotspot whose connectivity to cortical lesions is significantly ($p < 0.05$) associated with loss of consciousness from Snider et al. (2020).

pharmacological stimulation of the VTA (Giacino et al. 2012) have generally yielded more robust behavioral responses in patients with DoC than did transcranial magnetic stimulation or transcranial direct current stimulation (Fan et al. 2022; Thibaut et al. 2014; Wan et al. 2024) of cortical nodes. Our connectivity maps provide a potential mechanistic basis for these clinical trial results, as the CL and VTA were each found to be correlated to four cortical networks: DMN, SN, DAN, and VN in the CL, and DMN, ECN, SN, and VN in the VTA.

Notably, while a subcortical region of 4-network correlated activity showed substantial spatial overlap in the CL using the Iglesias atlas (Figure 5), this finding was only present in the left CL. We propose that this asymmetry is due to hemispheric heterogeneities in the SN, whereby the left thalamus has significantly higher connectivity values than does the right thalamus ($p < 0.001$ Mann–Whitney $U$ test). However, the right CL correlated highly with three networks (DMN, DAN, and VN), indicating that the CL has bilateral network hub properties (Figure S4). Interestingly, the correlated hub in the left CL additionally had a subregion of 2-network anticorrelated overlap, meaning that part of the CL represented a 6-network mixed hub (Figure S3). While the VTA's 4-network correlated hub did not overlap with additional anticorrelated networks, there were regions within the VTA that overlapped with a 5-network mixed hub consisting of three correlated networks and two anticorrelated networks (Figure S5). These observations reveal highly specialized subregions of subcortical hubs that may differentially modulate cortical networks via activating and inhibitory signaling.

The physiologic meaning of rs-fMRI anticorrelations within functional networks continues to be debated (Fox et al. 2005; Kevin and Michael 2017), and the microscale synaptic correlates of mesoscale anticorrelations remain unclear (DeFelipe 2010). Elucidating the therapeutic potential of a correlated hub versus that of a mixed hub, therefore, requires further inquiry in studies that link mesoscale neuroimaging

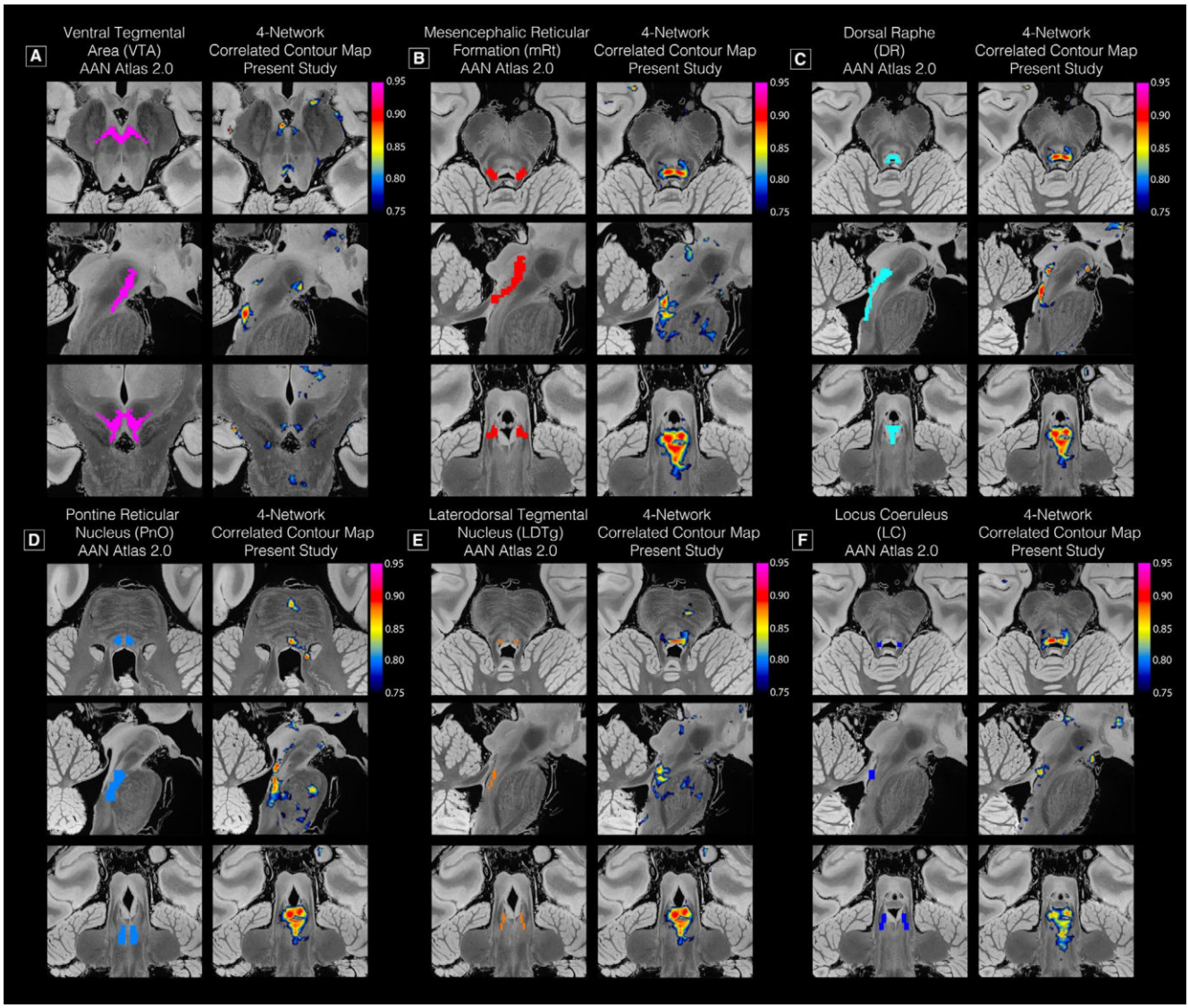


**FIGURE 8** | Comparison of our 4-network contour map with the nuclei defined in the Ascending Arousal Network (AAN) Atlas, version 2.0 2024. (A–F) corresponds to the VTA, mRt, DR, PnO, LDTg, and LC, respectively. Each panel has two columns with axial, sagittal, and coronal views of the pons and midbrain.

**TABLE 2** | The relationships between large-scale resting state brain networks and AAN nuclei.

| Nucleus | DMN | ECN | DAN | SN | VN | SMN |
|---|---|---|---|---|---|---|
| PnO | Correlated | Correlated | Correlated | Correlated | Correlated | |
| LC | Correlated | Correlated | Anticorrelated | Correlated | Correlated | Anticorrelated |
| LDTG | Correlated | Correlated | Anticorrelated | Correlated | Correlated | Anticorrelated |
| VTA | Correlated | Correlated | | Correlated | Correlated | |
| MnR | Correlated | Mixed | Mixed | Correlated | Correlated | Anticorrelated |
| DR | Correlated | Correlated | Anticorrelated | Correlated | Correlated | Anticorrelated |

*Note:* The "Correlated" relationship indicates that the network's connectivity values lie in the top 20% of the overall connectivity distribution within the nucleus. The "Anticorrelated" relationship indicates the counterpart for connectivity within the bottom 20% of the distribution. The "Mixed" relationship indicates both correlated and anticorrelated conditions occur within the same nucleus but in different spatial locations. An empty cell indicates no significant correlation was observed.

with microscale electrophysiology measures. Nevertheless, our functional connectivity maps are consistent with electrophysiologic studies showing a "funnel effect" of information processing in the human brain, whereby information dimensionality is reduced within subcortical structures (Blouw et al. 2016; Bota et al. 2015) such that stimulating a small hub

node in the subcortex generates widespread activation of the cortex (Horn et al. 2017, 2019). By beginning to link rs-fMRI connectivity maps to prior patterns observed in electrophysiologic data, our findings highlight the potential for rs-fMRI to serve as a clinically relevant tool that can identify subcortical therapeutic targets in patients with DoC.

The functional connectivity maps generated here, which we release to the academic community, expand the repertoire of therapeutic targets that can be considered in future clinical trials. While the central thalamus has been the most common target of electrophysiologic and ultrasonic therapies, and while the VTA has been the most common target of pharmacologic therapies, our findings suggest that hub nodes in the basal ganglia, medial temporal lobe, and BNST warrant future consideration as therapeutic targets in studies that aim to modulate cognition, behavior, and sensorimotor function in patients with severe brain injuries. Ultrasonic stimulation studies in patients with DoC have begun to target the basal ganglia (Cain, Visagan, et al. 2021) based on the mesocircuit hypothesis of consciousness (Schiff 2010), in which a striato-pallido-thalamic circuit is postulated to modulate a broad expanse of fronto-parietal cortex. The mechanistic relationships of the caudate and putamen hubs identified here to the mesocircuit are beyond the scope of the present work, but our findings add to growing evidence that it may be possible to identify the functional integrity of the mesocircuit using ultra-high resolution rs-fMRI (Li, Curley, et al. 2021), an advance that would have substantial implications for personalized therapy selection in patients with DoC who have a disrupted mesocircuit.

Although mesoscale measurements of functional connectivity are only surrogate markers of microscale signaling at the synaptic level, our identification of correlated, anticorrelated, and mixed hubs sheds new light on how subcortical ensembles of neurons may differentially modulate cortical networks. We found that subcortical hubs in the brainstem tegmentum and central thalamus had high levels of correlated connectivity with four or more cortical networks. These regions were consistently correlated with the DMN, SN, and VN, anticorrelated with the SMN, and had mixed connectivity properties with the DAN and ECN. In contrast, the BNST contained high levels of network overlap but with varying degrees (top 5% for SN, ECN, VN, DAN, and bottom 5% for the DMN and SMN) representing a mixed hub node that has the highest level of correlated activity from four networks and the highest level of anticorrelated activity from two networks. A region within the anterior putamen had the same mixed type of integration pattern as the BNST (correlated to the SN, ECN, VN, DAN, and anticorrelated to SMN and DMN) but with a lower threshold. Future studies combining rs-fMRI and intracranial electrophysiologic recordings are needed to elucidate the biological basis of mixed subcortical hubs (Stieger et al. 2024). We postulate that a subcortical node correlated with four task-positive networks and anticorrelated with the task-negative DMN may contribute to the brain's ability to "toggle" between task-positive and task-negative (i.e., resting) states.

Our observations about functional connectivity hubs in the healthy, conscious human brain also provide a mechanistic basis for previous descriptions of subcortical lesions that cause coma in patients with severe brain injuries. Specifically, we identified a subcortical hub that includes multiple reticular and extrareticular arousal nuclei and that is located in the same "hot spot" region of the pontomesencephalic tegmentum that was found in prior lesion studies to cause coma (Fischer et al. 2016; Parvizi and Damasio 2003) or to be associated with loss of consciousness (Snider et al. 2020). While the pathophysiologic mechanism of coma onset in patients with brainstem lesions continues to be debated, our functional connectivity results indicate that injury to a subcortical hub causes deafferentation and downregulation of cortical networks, such as the DMN, that are essential for consciousness. Given that recovery of consciousness after severe brain injury is associated with the reemergence of multiple cortical networks (Demertzi et al. 2015), a key area for future inquiry will be to identify the combinations of subcortical hubs and their associated cortical networks that are necessary and sufficient for recovery of consciousness.

Several limitations should be considered when interpreting these results in the context of future clinical trials that aim to restore consciousness after severe brain injury. First, as we did not include the limbic network, we may have failed to identify hubs or underestimated the degree of hubness within anatomic regions that are highly connected to the limbic network. Future studies may identify additional subcortical hubs in limbic regions such as the hippocampus, amygdala, nucleus accumbens, hypothalamus, or anterior nucleus of the thalamus (Catani et al. 2013). While some subcortical hubs identified here have been previously associated with consciousness, we also identified widely connected subcortical hubs in the basal ganglia, medial temporal lobe, and BNST that are historically associated with cognition, behavior, and sensorimotor function, not conscious awareness. For example, we found high levels of network overlap bilaterally within the caudate head for four networks when thresholding to include the top 2% of values, five networks when thresholding to the top 10%, and even a bilateral cluster of voxels of six network correlated overlap when thresholding to the top 15% of values. While lesions within the caudate can cause cognitive and behavioral dysfunction (Bokura and Robinson 1997; Graff-Radford et al. 2017; Mendez et al. 1989), to the best of our knowledge, there have been no associations between caudate lesions and loss of consciousness. For this reason, it is important to consider that the identification of a widely connected subcortical hub via rs-fMRI data does not prove that the hub modulates consciousness. Rather, these connectivity data must be interpreted in the context of prior animal and human studies that have linked each subcortical hub to distinct aspects of consciousness, cognition, behavior, or sensorimotor function.

To elucidate the connectivity properties of subcortical hubs that modulate conscious awareness, as compared to those that modulate cognition and behavior, it will be important for future studies to characterize these hubs as "bottom-up" activators of the cortex, or "top-down" recipients of cortical signals. In non-human primates, the caudate has been shown to receive inputs from multiple cortical networks, including from the dorsolateral prefrontal cortex (ECN), the dorsal anterior cingulate (DMN), and the anterior cingulate (SN) (Haber 2016). Conversely, animal models indicate that other subcortical hub regions identified in this study, such as the intralaminar nuclei of the thalamus and

the brainstem's arousal nuclei, send ascending axonal projections to the cortex (Azmitia and Gannon 1986). Building upon these animal structural connectivity data, there is a need to characterize the functional properties of subcortical hubs in humans by using dynamic rs-fMRI and intracranial electrophysiologic recordings to determine whether resting state activity in a subcortical region precedes or follows cortical network activity (Setzer et al. 2022) (Khalaf et al. 2025) (Edlow et al. 2024; Stieger et al. 2024). For dynamic rs-fMRI lag analyses, there has historically been a methodologic trade-off whereby achieving ultra-high temporal resolution (e.g., TR = 247 ms in Setzer et al. 2022) requires decreasing the spatial resolution or limiting the number of imaging slices, which precludes whole-brain coverage. Future studies aiming to characterize the "bottom-up" versus "top-down" signaling properties of subcortical connectivity hubs will therefore need to balance these trade-offs between temporal and spatial resolution.

Another methodological limitation of the present work is that the identification of subcortical hubs at the group level requires precise registration across subjects, which was enabled here by the NASCAR network identification pipeline (Li, Curley, et al. 2021). Recent work based on deep neural network methods has been shown to improve inter-subject registration (Balakrishnan et al. 2019; Cheng et al. 2020), but the registration of subcortical structures remains challenging due to the low resolution and low SNR of the rs-fMRI data, as well as the potential mismatch between human brain anatomy and function (Li et al. 2024). Therefore, inferences should not be made on any results reported here at voxel resolution. For instance, Figure 3 illustrates hubs that are consistently located within the hippocampus across multiple networks. The small overlap in the amygdala, although also across multiple networks, may not provide sufficiently strong evidence of hubness because of potentially inaccurate inter-subject registration. Given the possibility of distortions within the brainstem due to its proximity to air-tissue boundaries (Brooks et al. 2013), advances in distortion correction are also needed to improve the anatomic precision and robustness of brainstem hub identification.

In conclusion, we identified subcortical connectivity hubs in the VTA, CL, and Pf—regions that have historically been targeted in therapeutic trials to restore consciousness in patients with severe brain injuries. An additional hub within the pontomesencephalic tegmentum overlapped with a previously described coma-causing "hot spot," indicating that this brainstem region is a potential therapeutic target for neuromodulation of consciousness. Subcortical hubs were also identified in regions of the caudate, putamen, medial temporal lobe, and BNST that are believed to modulate cognition, behavior, and sensorimotor function. While further evidence from multimodal neuroimaging and electrophysiologic studies is needed to elucidate the specific functional role of each subcortical hub, these results strengthen the evidence base for targeting subcortical hubs as a therapeutic strategy to restore consciousness in patients with DoC.

### Author Contributions

B.L.E., J.L. and M.K.C. conceived and designed the study. M.K.C., J.L. and B.L.E. wrote the original draft of the manuscript. M.K.C. and J.L. processed and analyzed the data. A.H. and L.D.L. contributed to the study design and interpreted the data. B.L.E. and J.L. contributed to project administration and supervision. All authors contributed to editing the manuscript.


### Acknowledgments

The authors thank Drs. David Fischer and Samuel B. Snider for providing the neuroanatomic coordinates of their brainstem hotspots for comparison to the results in the present study.


### Ethics Statement

The authors have nothing to report.

### Consent

The authors have nothing to report.

### Conflicts of Interest

A.H. reports lecture fees for Boston Scientific, is a consultant for Modulight.bio, was a consultant for FxNeuromodulation and Abbott in recent years and serves as a co-inventor on a patent granted to Charité University Medicine Berlin that covers multisymptom DBS fiberfiltering and an automated DBS parameter suggestion algorithm unrelated to this work (patent #LU103178).

### Data Availability Statement

The data used in this study are publicly available from the Wash U/U Minn component of the Human Connectome Project, Young Adult Study at https://www.humanconnectome.org/study/hcp-young-adult. For research purposes, we release the code at the GitHub repository (https://github.com/ComaRecoveryLab/Subcortical_Network_Hubs).

### References


Akrami, H., A. Joshi, J. Li, and R. Leahy. 2019. "Group-Wise Alignment of Resting fMRI in Space and Time." (Vol. 10949). SPIE. https://doi.org/10.1117/12.2512564.

Aston-Jones, G., S. Chen, Y. Zhu, and M. L. Oshinsky. 2001. "A Neural Circuit for Circadian Regulation of Arousal." *Nature Neuroscience* 4, no. 7: 732–738. https://doi.org/10.1038/89522.

Azmitia, E. C., and P. J. Gannon. 1986. "The Primate Serotonergic System: A Review of Human and Animal Studies and a Report on *Macaca fascicularis*." *Advances in Neurology* 43: 407–468. https://www.ncbi.nlm.nih.gov/pubmed/2418648.

Balakrishnan, G., A. Zhao, M. R. Sabuncu, J. Guttag, and A. V. Dalca. 2019. "VoxelMorph: A Learning Framework for Deformable Medical Image Registration." *IEEE Transactions on Medical Imaging* 38: 1788–1800. https://doi.org/10.1109/TMI.2019.2897538.

Blouw, P., E. Solodkin, P. Thagard, and C. Eliasmith. 2016. "Concepts as Semantic Pointers: A Framework and Computational Model." *Cognitive Science* 40, no. 5: 1128–1162. https://doi.org/10.1111/cogs.12265.

Bokura, H., and R. G. Robinson. 1997. "Long-Term Cognitive Impairment Associated With Caudate Stroke." *Stroke* 28, no. 5: 970–975. https://doi.org/10.1161/01.str.28.5.970.

Bota, M., O. Sporns, and L. W. Swanson. 2015. "Architecture of the Cerebral Cortical Association Connectome Underlying Cognition." *Proceedings of the National Academy of Sciences of the United States of America* 112, no. 16: E2093–E2101. https://doi.org/10.1073/pnas.1504394112.

Brooks, J. C., O. K. Faull, K. T. Pattinson, and M. Jenkinson. 2013. "Physiological Noise in Brainstem FMRI." *Frontiers in Human Neuroscience* 7: 623. https://doi.org/10.3389/fnhum.2013.00623.

Cain, J. A., N. M. Spivak, J. P. Coetzee, et al. 2021. "Ultrasonic Thalamic Stimulation in Chronic Disorders of Consciousness." *Brain Stimulation* 14, no. 2: 301–303. https://doi.org/10.1016/j.brs.2021.01.008.

Cain, J. A., N. M. Spivak, J. P. Coetzee, et al. 2022. "Ultrasonic Deep Brain Neuromodulation in Acute Disorders of Consciousness: A Proof-of-Concept." *Brain Sciences* 12, no. 4: 428. https://doi.org/10.3390/brainsci12040428.

Cain, J. A., S. Visagan, M. A. Johnson, et al. 2021. "Real Time and Delayed Effects of Subcortical Low Intensity Focused Ultrasound." *Scientific Reports* 11, no. 1: 6100. https://doi.org/10.1038/s41598-021-85504-y.

Catani, M., F. Dell'acqua, and M. Thiebaut de Schotten. 2013. "A Revised Limbic System Model for Memory, Emotion and Behaviour." *Neuroscience and Biobehavioral Reviews* 37, no. 8: 1724–1737. https://doi.org/10.1016/j.neubiorev.2013.07.001.

Cheng, J., A. V. Dalca, B. Fischl, L. Zollei, and Alzheimer's Disease Neuroimaging Initiative. 2020. "Cortical Surface Registration Using Unsupervised Learning." *NeuroImage* 221: 117161. https://doi.org/10.1016/j.neuroimage.2020.117161.

Chudy, D., V. Deletis, F. Almahariq, P. Marcinkovic, J. Skrlin, and V. Paradzik. 2018. "Deep Brain Stimulation for the Early Treatment of the Minimally Conscious State and Vegetative State: Experience in 14 Patients." *Journal of Neurosurgery* 128, no. 4: 1189–1198. https://doi.org/10.3171/2016.10.JNS161071.

Chudy, D., V. Deletis, V. Paradzik, et al. 2023. "Deep Brain Stimulation in Disorders of Consciousness: 10 Years of a Single Center Experience." *Scientific Reports* 13, no. 1: 19491. https://doi.org/10.1038/s41598-023-46300-y.

Crossley, N. A., A. Mechelli, J. Scott, et al. 2014. "The Hubs of the Human Connectome Are Generally Implicated in the Anatomy of Brain Disorders." *Brain* 137, no. Pt 8: 2382–2395. https://doi.org/10.1093/brain/awu132.

DeFelipe, J. 2010. "From the Connectome to the Synaptome: An Epic Love Story." *Science* 330, no. 6008: 1198–1201. https://doi.org/10.1126/science.1193378.

Demertzi, A., G. Antonopoulos, L. Heine, et al. 2015. "Intrinsic Functional Connectivity Differentiates Minimally Conscious From Unresponsive Patients." *Brain* 138, no. Pt 9: 2619–2631. https://doi.org/10.1093/brain/awv169.

Edlow, B. L., M. E. Barra, D. W. Zhou, et al. 2020. "Personalized Connectome Mapping to Guide Targeted Therapy and Promote Recovery of Consciousness in the Intensive Care Unit." *Neurocritical Care* 33, no. 2: 364–375. https://doi.org/10.1007/s12028-020-01062-7.

Edlow, B. L., J. Claassen, N. D. Schiff, and D. M. Greer. 2021. "Recovery From Disorders of Consciousness: Mechanisms, Prognosis and Emerging Therapies." *Nature Reviews. Neurology* 17, no. 3: 135–156. https://doi.org/10.1038/s41582-020-00428-x.

Edlow, B. L., R. L. Haynes, E. Takahashi, et al. 2013. "Disconnection of the Ascending Arousal System in Traumatic Coma." *Journal of Neuropathology and Experimental Neurology* 72, no. 6: 505–523. https://doi.org/10.1097/NEN.0b013e3182945bf6.

Edlow, B. L., A. Mareyam, A. Horn, et al. 2019. "7 Tesla MRI of the Ex Vivo Human Brain at 100 Micron Resolution." *Scientific Data* 6. https://doi.org/10.1038/s41597-019-0254-8.

Edlow, B. L., M. Olchanyi, H. J. Freeman, et al. 2024. "Multimodal MRI Reveals Brainstem Connections That Sustain Wakefulness in Human Consciousness." *Science Translational Medicine* 16, no. 745: eadj4303. https://doi.org/10.1126/scitranslmed.adj4303.

Edlow, B. L., L. R. D. Sanz, L. Polizzotto, et al. 2021. "Therapies to Restore Consciousness in Patients With Severe Brain Injuries: A Gap Analysis and Future Directions." *Neurocritical Care* 35, no. Suppl 1: 68–85. https://doi.org/10.1007/s12028-021-01227-y.

Elias, G. J. B., A. Loh, D. Gwun, et al. 2021. "Deep Brain Stimulation of the Brainstem." *Brain* 144, no. 3: 712–723. https://doi.org/10.1093/brain/awaa374.

Fan, J., Y. Zhong, H. Wang, N. Aierken, and R. He. 2022. "Repetitive Transcranial Magnetic Stimulation Improves Consciousness in Some Patients With Disorders of Consciousness." *Clinical Rehabilitation* 36, no. 7: 916–925. https://doi.org/10.1177/02692155221089455.

Fischer, D. B., A. D. Boes, A. Demertzi, et al. 2016. "A Human Brain Network Derived From Coma-Causing Brainstem Lesions." *Neurology* 87, no. 23: 2427–2434. https://doi.org/10.1212/WNL.0000000000003404.

Fox, M. D., A. Z. Snyder, J. L. Vincent, M. Corbetta, D. C. Van Essen, and M. E. Raichle. 2005. "The Human Brain Is Intrinsically Organized Into Dynamic, Anticorrelated Functional Networks." *Proceedings of the National Academy of Sciences of the United States of America* 102, no. 27: 9673–9678. https://doi.org/10.1073/pnas.0504136102.

Fridman, E. A., J. R. Osborne, P. D. Mozley, J. D. Victor, and N. D. Schiff. 2019. "Presynaptic Dopamine Deficit in Minimally Conscious State Patients Following Traumatic Brain Injury." *Brain* 142, no. 7: 1887–1893. https://doi.org/10.1093/brain/awz118.

Fuller, P. M., D. Sherman, N. P. Pedersen, C. B. Saper, and J. Lu. 2011. "Reassessment of the Structural Basis of the Ascending Arousal System." *Journal of Comparative Neurology* 519, no. 5: 933–956. https://doi.org/10.1002/cne.22559.

Giacino, J. T., J. Whyte, E. Bagiella, et al. 2012. "Placebo-Controlled Trial of Amantadine for Severe Traumatic Brain Injury." *New England Journal of Medicine* 366, no. 9: 819–826. https://doi.org/10.1056/NEJMoa1102609.

Girn, M., R. Setton, G. R. Turner, and R. N. Spreng. 2024. "The 'Limbic Network,' Comprising Orbitofrontal and Anterior Temporal Cortex, Is Part of an Extended Default Network: Evidence From Multi-Echo fMRI." *Network Neuroscience* 8, no. 3: 860–882. https://doi.org/10.1162/netn_a_00385.

Glasser, M. F., S. M. Smith, D. S. Marcus, et al. 2016. "The Human Connectome Project's Neuroimaging Approach." *Nature Neuroscience* 19, no. 9: 1175–1187. https://doi.org/10.1038/nn.4361.

Glasser, M. F., S. N. Sotiropoulos, J. A. Wilson, et al. 2013. "The Minimal Preprocessing Pipelines for the Human Connectome Project." *NeuroImage* 80: 105–124. https://doi.org/10.1016/j.neuroimage.2013.04.127.

Graff-Radford, J., L. Williams, D. T. Jones, and E. E. Benarroch. 2017. "Caudate Nucleus as a Component of Networks Controlling Behavior." *Neurology* 89, no. 21: 2192–2197. https://doi.org/10.1212/WNL.0000000000004680.

Haber, S. N. 2016. "Corticostriatal Circuitry." *Dialogues in Clinical Neuroscience* 18, no. 1: 7–21. https://doi.org/10.31887/DCNS.2016.18.1/shaber.

Horn, A., and M. D. Fox. 2020. "Opportunities of Connectomic Neuromodulation." *NeuroImage* 221: 117180. https://doi.org/10.1016/j.neuroimage.2020.117180.

Horn, A., M. Reich, J. Vorwerk, et al. 2017. "Connectivity Predicts Deep Brain Stimulation Outcome in Parkinson Disease." *Annals of Neurology* 82, no. 1: 67–78. https://doi.org/10.1002/ana.24974.

Horn, A., G. Wenzel, F. Irmen, et al. 2019. "Deep Brain Stimulation Induced Normalization of the Human Functional Connectome in Parkinson's Disease." *Brain* 142, no. 10: 3129–3143. https://doi.org/10.1093/brain/awz239.

Hutchison, R. M., T. Womelsdorf, E. A. Allen, et al. 2013. "Dynamic Functional Connectivity: Promise, Issues, and Interpretations." *NeuroImage* 80: 360–378. https://doi.org/10.1016/j.neuroimage.2013.05.079.

Iglesias, J. E., R. Insausti, G. Lerma-Usabiaga, et al. 2018. "A Probabilistic Atlas of the Human Thalamic Nuclei Combining Ex Vivo MRI and

Histology." *NeuroImage* 183: 314–326. https://doi.org/10.1016/j.neuroimage.2018.08.012.

Joshi, A. A., M. Chong, J. Li, et al. 2018. "Are You Thinking What I'm Thinking? Synchronization of Resting fMRI Time-Series Across Subjects." *NeuroImage* 172: 740–752. https://doi.org/10.1016/j.neuroimage.2018.01.058.

Karahanoglu, F. I., and D. Van De Ville. 2015. "Transient Brain Activity Disentangles fMRI Resting-State Dynamics in Terms of Spatially and Temporally Overlapping Networks." *Nature Communications* 6: 7751. https://doi.org/10.1038/ncomms8751.

Kevin, M., and D. F. Michael. 2017. "Towards a Consensus Regarding Global Signal Regression for Resting State Functional Connectivity MRI." *NeuroImage* 154: 169–173. https://doi.org/10.1016/j.neuroimage.2016.11.052.

Khalaf, A., E. Lopez, J. Li, A. Horn, B. L. Edlow, and H. Blumenfeld. 2025. "Shared Subcortical Arousal Systems Across Sensory Modalities During Transient Modulation of Attention." *NeuroImage* 312: 121224. https://doi.org/10.1016/j.neuroimage.2025.121224.

Koch, C., M. Massimini, M. Boly, and G. Tononi. 2016. "Neural Correlates of Consciousness: Progress and Problems." *Nature Reviews. Neuroscience* 17, no. 5: 307–321. https://doi.org/10.1038/nrn.2016.22.

Koike, S., S. C. Tanaka, T. Okada, et al. 2021. "Brain/MINDS Beyond Human Brain MRI Project: A Protocol for Multi-Level Harmonization Across Brain Disorders Throughout the Lifespan." *NeuroImage: Clinical* 30: 102600. https://doi.org/10.1016/j.nicl.2021.102600.

Lee, M. H., C. D. Smyser, and J. S. Shimony. 2013. "Resting-State fMRI: A Review of Methods and Clinical Applications." *AJNR. American Journal of Neuroradiology* 34, no. 10: 1866–1872. https://doi.org/10.3174/ajnr.A3263.

Leech, R., R. Braga, and D. J. Sharp. 2012. "Echoes of the Brain Within the Posterior Cingulate Cortex." *Journal of Neuroscience* 32, no. 1: 215–222. https://doi.org/10.1523/JNEUROSCI.3689-11.2012.

Lemon, R. N., and S. A. Edgley. 2010. "Life Without a Cerebellum." *Brain* 133, no. Pt 3: 652–654. https://doi.org/10.1093/brain/awq030.

Li, J., S. Choi, A. A. Joshi, J. L. Wisnowski, and R. M. Leahy. 2018. "Global Pdf-Based Temporal Non-Local Means Filtering Reveals Individual Differences in Brain Connectivity." *Proceedings/ IEEE International Symposium on Biomedical Imaging* 2018: 15–19. https://doi.org/10.1109/ISBI.2018.8363513.

Li, J., W. H. Curley, B. Guerin, et al. 2021. "Mapping the Subcortical Connectivity of the Human Default Mode Network." *NeuroImage* 245: 118758. https://doi.org/10.1016/j.neuroimage.2021.118758.

Li, J., Y. Liu, J. L. Wisnowski, and R. M. Leahy. 2023. "Identification of Overlapping and Interacting Networks Reveals Intrinsic Spatiotemporal Organization of the Human Brain." *NeuroImage* 270: 119944. https://doi.org/10.1016/j.neuroimage.2023.119944.

Li, J., G. Tuckute, E. Fedorenko, B. L. Edlow, A. V. Dalca, and B. Fischl. 2024. "JOSA: Joint Surface-Based Registration and Atlas Construction of Brain Geometry and Function." *Medical Image Analysis* 98: 103292. https://doi.org/10.1016/j.media.2024.103292.

Li, J., J. L. Wisnowski, A. A. Joshi, and R. M. Leahy. 2021. "Robust Brain Network Identification From Multi-Subject Asynchronous fMRI Data." *NeuroImage* 227: 117615. https://doi.org/10.1016/j.neuroimage.2020.117615.

Luppi, A. I., H. M. Gellersen, Z. Q. Liu, et al. 2024. "Systematic Evaluation of fMRI Data-Processing Pipelines for Consistent Functional Connectomics." *Nature Communications* 15, no. 1: 4745. https://doi.org/10.1038/s41467-024-48781-5.

Mendez, M. F., N. L. Adams, and K. S. Lewandowski. 1989. "Neurobehavioral Changes Associated With Caudate Lesions." *Neurology* 39, no. 3: 349–354. https://doi.org/10.1212/wnl.39.3.349.

Moruzzi, G., and H. W. Magoun. 1949. "Brain Stem Reticular Formation and Activation of the EEG." *Electroencephalography and Clinical Neurophysiology* 1, no. 4: 455–473. https://www.ncbi.nlm.nih.gov/pubmed/18421835.

Pais-Roldan, P., B. L. Edlow, Y. Jiang, J. Stelzer, M. Zou, and X. Yu. 2019. "Multimodal Assessment of Recovery From Coma in a Rat Model of Diffuse Brainstem Tegmentum Injury." *NeuroImage* 189: 615–630. https://doi.org/10.1016/j.neuroimage.2019.01.060.

Parvizi, J. 2003. "Neuroanatomical Correlates of Brainstem Coma." *Brain* 126, no. 7: 1524–1536. https://doi.org/10.1093/brain/awg166.

Parvizi, J., and A. R. Damasio. 2003. "Neuroanatomical Correlates of Brainstem Coma." *Brain* 126, no. 7: 1524–1536. https://doi.org/10.1093/brain/awg166.

Raichle, M. E. 2011. "The Restless Brain." *Brain Connectivity* 1, no. 1: 3–12. https://doi.org/10.1089/brain.2011.0019.

Redinbaugh, M. J., J. M. Phillips, N. A. Kambi, et al. 2020. "Thalamus Modulates Consciousness via Layer-Specific Control of Cortex." *Neuron* 106, no. 1: 66–75.e12. https://doi.org/10.1016/j.neuron.2020.01.005.

Scammell, T. E., E. Arrigoni, and J. O. Lipton. 2017. "Neural Circuitry of Wakefulness and Sleep." *Neuron* 93, no. 4: 747–765. https://doi.org/10.1016/j.neuron.2017.01.014.

Schiff, N. D. 2010. "Recovery of Consciousness After Brain Injury: A Mesocircuit Hypothesis." *Trends in Neurosciences* 33, no. 1: 1–9. https://doi.org/10.1016/j.tins.2009.11.002.

Schiff, N. D., J. T. Giacino, K. Kalmar, et al. 2007. "Behavioural Improvements With Thalamic Stimulation After Severe Traumatic Brain Injury." *Nature* 448, no. 7153: 600–603. https://doi.org/10.1038/nature06041.

Seeley, W. W., V. Menon, A. F. Schatzberg, et al. 2007. "Dissociable Intrinsic Connectivity Networks for Salience Processing and Executive Control." *Journal of Neuroscience* 27, no. 9: 2349–2356. https://doi.org/10.1523/JNEUROSCI.5587-06.2007.

Setzer, B., N. E. Fultz, D. E. P. Gomez, et al. 2022. "A Temporal Sequence of Thalamic Activity Unfolds at Transitions in Behavioral Arousal State." *Nature Communications* 13, no. 1: 5442. https://doi.org/10.1038/s41467-022-33010-8.

Smith, S. M., C. F. Beckmann, J. Andersson, et al. 2013. "Resting-State fMRI in the Human Connectome Project." *NeuroImage* 80: 144–168. https://doi.org/10.1016/j.neuroimage.2013.05.039.

Snider, S. B., J. Hsu, R. R. Darby, et al. 2020. "Cortical Lesions Causing Loss of Consciousness Are Anticorrelated With the Dorsal Brainstem." *Human Brain Mapping* 41, no. 6: 1520–1531. https://doi.org/10.1002/hbm.24892.

Steriade, M., and L. L. Glenn. 1982. "Neocortical and Caudate Projections of Intralaminar Thalamic Neurons and Their Synaptic Excitation From Midbrain Reticular Core." *Journal of Neurophysiology* 48, no. 2: 352–371. https://doi.org/10.1152/jn.1982.48.2.352.

Stieger, J. R., P. Pinheiro-Chagas, Y. Fang, et al. 2024. "Cross-Regional Coordination of Activity in the Human Brain During Autobiographical Self-Referential Processing." *Proceedings of the National Academy of Sciences of the United States of America* 121, no. 32: e2316021121. https://doi.org/10.1073/pnas.2316021121.

Tasserie, J., L. Uhrig, J. D. Sitt, et al. 2022. "Deep Brain Stimulation of the Thalamus Restores Signatures of Consciousness in a Nonhuman Primate Model." *Science Advances* 8, no. 11: eabl5547. https://doi.org/10.1126/sciadv.abl5547.

Thibaut, A., M. A. Bruno, D. Ledoux, A. Demertzi, and S. Laureys. 2014. "tDCS in Patients With Disorders of Consciousness: Sham-Controlled Randomized Double-Blind Study." *Neurology* 82, no. 13: 1112–1118. https://doi.org/10.1212/WNL.0000000000000260.

van den Heuvel, M. P., and O. Sporns. 2013. "Network Hubs in the Human Brain." *Trends in Cognitive Sciences* 17, no. 12: 683–696. https://doi.org/10.1016/j.tics.2013.09.012.

Vertes, R. P., and G. F. Martin. 1988. "Autoradiographic Analysis of Ascending Projections From the Pontine and Mesencephalic Reticular Formation and the Median Raphe Nucleus in the Rat." *Journal of Comparative Neurology* 275, no. 4: 511–541. https://doi.org/10.1002/cne.902750404.

Wan, X., Y. Zhang, Y. Li, and W. Song. 2024. "Effects of Parietal Repetitive Transcranial Magnetic Stimulation in Prolonged Disorders of Consciousness: A Pilot Study." *Heliyon* 10, no. 9: e30192. https://doi.org/10.1016/j.heliyon.2024.e30192.

Whyte, J., R. Rajan, A. Rosenbaum, et al. 2014. "Zolpidem and Restoration of Consciousness." *American Journal of Physical Medicine & Rehabilitation* 93, no. 2: 101–113. https://doi.org/10.1097/PHM.0000000000000069.

Yeo, B. T., F. M. Krienen, J. Sepulcre, et al. 2011. "The Organization of the Human Cerebral Cortex Estimated by Intrinsic Functional Connectivity." *Journal of Neurophysiology* 106, no. 3: 1125–1165. https://doi.org/10.1152/jn.00338.2011.

## Supporting Information

Additional supporting information can be found online in the Supporting Information section. **Data S1:** hbm70352-sup-0001-Supinfo.docx. **Video S1:** The correlated network voxel distributions (top 5% of values) for each of the six networks are shown at descending axial slices through the subcortex.